This article has been accepted for publication in a future issue of this journal, but has not been fully edited. Content may change prior to final publication. Citation information: DOI 10.1109/JSEN.2019.2962610, IEEE Sensors Journal

Reflected light intensity-modulated continuous liquid level sensor based on oblique end face coupling optical fibers

Junfeng Ge, *Member, IEEE,* Xin Cheng, Chengrui Zhao, Kang Gui, Wei Zhang, Faouzi A. Cheikh and Lin Ye

***Abstract*—A light intensity-modulated optical fiber sensor for continuous level measurement is proposed and demonstrated. The sensor is constructed by vertically arranging groups of fibers on the oblique surface which reflects all the incident light when the fibers are in the air but a small proportion of light when the fibers are immersed in the liquid. In order to implement easy modulation and detection, the angle of oblique surface is specially designed to get the maximum intensity modulation according to Fresnel reflection. The fiber groups consist of emitting and receiving fibers, which are tightly fixed to make it easy to detect reflected light based on side coupling effect. The calculation model of the oblique structure and the light path simulation by finite element analysis are used to optimize the oblique angle and prove the feasibility of the sensor. Gradient level experiments and stability tests in the laboratory indicate that the sensor has high sensitivity of 0.21mW/cm, superior resolution and good stability.**

***Index Terms*—continuous liquid level measurement, Fresnel reflection, oblique end face fiber, maximum intensity modulation, side coupling.**

I. Introduction

LIQUID level measurement plays a fundamental and important role in many fields involved with liquid storage, liquid material supply and liquid level monitoring. In chemical industry, the volume ratio of reactants determines the results of reaction process. In aircraft, more accurate control of the fuel level [1] not only increases the aircraft effective payloads but also ensures a safer flight. The measurement of liquid level is in universal demand in all fields of life and production, especially in the industrial automation process, which requires both high accuracy and commendable adaptation to extraordinary circumstances. Considering the safety requirements for flammable and explosive environments, the optical fiber liquid level sensors have attracted lots of interests due to their distinguished advantages over the mechanical or electrical ones such as intrinsic safety, fast response, electromagnetic immunity, chemical erosion resistance, compact size and lightweight [2].

During the past decades, numerous optical fiber based liquid level sensors have been proposed. In general, these sensors can be categorized into two types, the discrete or point and the continuous liquid level sensors.

The discrete liquid level sensors are typically operated based on intensity modulation by measuring the optical power change in reflection or transmission through the sensor head. There are sensors with prisms [3]–[5], oblique end face fibers [6], semi-circle sintered fiber node [7], hemispherical fiber tip [8], angled and retroreflecting-type fiber tips [9].

The continuous liquid level sensors work on the principle of either wavelength modulation or intensity modulation. The well known wavelength modulation techniques include fiber Bragg gratings (FBGs), long period gratings (LPGs) and modal interferometer. FBGs are sensitive to surrounding liquid level variance assisted with post-processing techniques of removing a part of the fiber cladding by side-polishing [10], and hydrofluoric (HF) acid etching [11] or using tilted FBG [12] and hollow core FBG [13]. The LPGs have been demonstrated for liquid level sensing because of their inherent sensitivity to external refractive index (RI) by propagating core mode to cladding modes [14]–[16]. The sensors based on modal interferometer have been proposed with different structures. There are single-mode fiber (SMF) spliced to no-core fiber (NCF) with coated mirror at the other end [17], SMF-NCF-SMF [18], [19], SMF-dual side-hole fiber-SMF [20], SMF-HCF(hollow core fiber)-SMF [21], [22], SMF-NCF-D-shape fiber-NCF-SMF [23], SMF-MMF(multi-mode fiber)-thinned fiber-SMF [24],SMF-MMF-SMF [25] and MMF-NCF-MMF [26]. Although the sensitivities of the wavelength-modulated sensors are high, the wavelength processing depends on complicated technology or instruments like optical spectrum analyzer (OSA) and their measurement ranges are limited to several centimeters including high cross response to temperature and RI.

The plastic optical fibers (POFs) are widely used in intensity-modulated liquid level sensors with much larger measurement range. The POFs can be decladded [27], removed with a portion of the core [28], twisted with scattering particles

Manuscript received ** **, 2019; revised ** **, 2019.(Corresponding author: Xin Cheng.)

This work was supported by National Key R&D Program of China(2016YFB1200401), the National Natural Science Foundation of China (Grant No. 61104202); the scholarship from China Scholarship Council and the Research Council of Norway.

J. Ge is with the School of Artificial Intelligence and Automation, Huazhong University of Science and Technology, Wuhan, 430074, China, and also with National Key Laboratory of Science and Technology on Multispectral Information Processing, Wuhan,430074, China (e-mail: gejf@hust.edu.cn)

C.Zhao is with the Research & Development Center, Ningbo CRRC Times Transducer Technology CO., LTD, Ningbo, 315021, China, zhaocr@csrzic.com)

X.Cheng, K.Gui and L.Ye are with the School of Artificial Intelligence and Automation, Huazhong University of Science and Technology, Wuhan, 430074, China,(e-mail: chengxi, gk_work, lye@hust.edu.cn)

W. Zhang is with Wuhan Second Ship Design and Research Institute, Wuhan, 430205, China (e-mail: 5709195@qq.com)

F. A. Cheikh is with Department of Computer Science, Norwegian University of Science and Technology, Gjøvik, 2815, Norway (e-mail: faouzi.cheikh@ntnu.no)

This article has been accepted for publication in a future issue of this journal, but has not been fully edited. Content may change prior to final publication. Citation information: DOI 10.1109/JSEN.2019.2962610, IEEE Sensors Journal

in the core [29], twisted with two coupled POFs [30] and glued with two parallel POFs [31]. However, the continuous liquid level sensors based on POFs usually have weak effective light signals and are susceptible to high temperature, which limits their applications in many fields.

In order to develop a liquid level sensor capable of working in harsh environments with large measurement range, inspired by our previous work [6], a novel light intensity-modulated oblique fiber continuous level sensor is proposed based on Fresnel reflection. The sensor has an oblique end face with two columns of oblique fibers, one as the emitting fibers and the other as the receiving fibers. The incident light in the emitting fibers is reflected back by the oblique end face and then is transversely coupled into receiving fibers. Different proportion of light will be reflected when the fibers are in the air and liquid. The specific angle of the oblique surface is designed based on Fresnel reflection to get maximum light intensity modulation. The feasibility of the structure is confirmed by finite element analysis of COMSOL Multiphysics simulation. A series of experiments have been carried out and the results verify that the sensor has high sensitivity and good stability.

II. Principle

The proposed continuous level sensor is based on intensity modulation of reflected light. When a light is incident on the surface between different medium, the light can be resolved into the combination of two orthogonal linear polarization components called S polarization and P polarization [32]. The S polarization refers to the wave component whose electric field normal to the plane of incidence and the magnetic field in the plane of incidence. The P polarization is the wave component orthogonal to S polarization. Described as Fresnel reflection [33] in Eq.(1), the effective reflection R_{eff} is the average of the two polarization coefficients R_s and R_p, which are determined by the RI of the exterior n_2 and the incident angle θ_i.

$$\begin{cases} R_s = \left|\dfrac{n_1\cos\theta_i - n_2\cos\theta_t}{n_1\cos\theta_i + n_2\cos\theta_t}\right|^2 = \left|\dfrac{n_1\cos\theta_i - n_2\sqrt{1-\left(\frac{n_1}{n_2}\sin\theta_i\right)^2}}{n_1\cos\theta_i + n_2\sqrt{1-\left(\frac{n_1}{n_2}\sin\theta_i\right)^2}}\right|^2 \\ R_p = \left|\dfrac{n_1\cos\theta_t - n_2\cos\theta_i}{n_1\cos\theta_t + n_2\cos\theta_i}\right|^2 = \left|\dfrac{n_1\sqrt{1-\left(\frac{n_1}{n_2}\sin\theta_i\right)^2} - n_2\cos\theta_i}{n_1\sqrt{1-\left(\frac{n_1}{n_2}\sin\theta_i\right)^2} + n_2\cos\theta_i}\right|^2 \\ R_{eff} = \dfrac{R_s + R_p}{2} \end{cases} \quad (1)$$

The prototype of the sensor is shown in Fig.1 and its oblique surface with groups of oblique fibers is vertically placed into liquid. The sensitive part consists of an oblique surface, light modulation and coupling segments and a cavity for fibers distribution. Each group of oblique emitting and receiving fibers works as a sensing unit. When liquid contacts the oblique surface, some groups of fibers are immersed and the light reflectance R_{liquid}, according to Fresnel reflection, is weaker than that of fibers in the air R_{air}. The more fibers are immersed, the smaller the total reflected light intensity is, summarized mathematically as Eq.(2), where H is the height of oblique surface and h is the height of the immersed

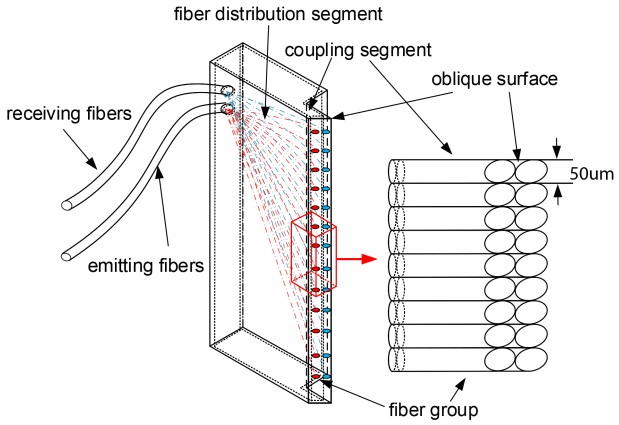

Fig. 1. Prototype of the continuous level sensor based on oblique end face fibers

surface. It is easy to deduce that it is the light reflectance difference of fibers in the air and fibers immersed in the liquid $R_{air} - R_{liquid}$ that determines the sensitivity of total reflected light R_{total} vs liquid level h. The light intensity modulation depth $M(\theta_i) = R_{air} - R_{liquid}$ is used to analyze the sensitivity, which is only related to θ_i after n_1, n_2 are determined. The influence of different RI of measured liquid n_2 will be discussed later by experiments. In order to implement a continuous level sensor with high sensitivity to level variance, the $M(\theta_i)$ should be as big as possible.

$$\begin{cases} R_{total} = R_{liquid} \times \dfrac{h}{H} + R_{air} \times \dfrac{H-h}{H} \\ \qquad\quad = R_{air} - \left(R_{air} - R_{liquid}\right) \times \dfrac{h}{H} \\ M(\theta_i) = R_{air} - R_{liquid} \end{cases} \quad (2)$$

The curve of $M(\theta_i)$ vs θ_i is shown in Fig.2 and the preferred value of $M(\theta_i)$ should be at the peak area. Because the incident light does not travel in line but in conical, the incident angle θ_i is always a range not a value. Hence, a relatively big θ_i variance range from $\theta_{i_{\min}}$ to $\theta_{i_{\max}}$ is selected, and $\theta_{i_{\min}} = 37.9°$ is the peak point of the curve.

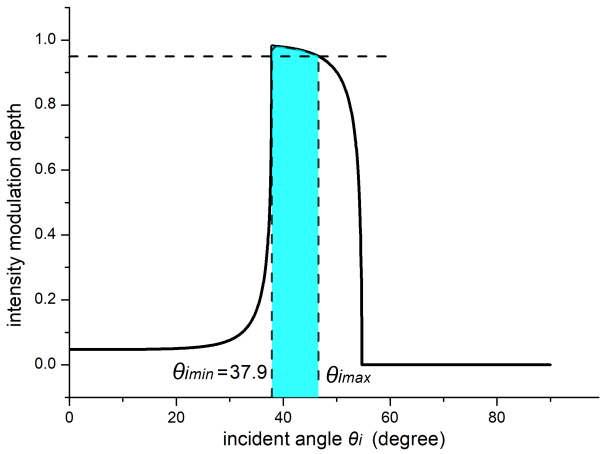

Fig. 2. Light intensity modulation depth vs incident angle when $n_1 = 1.63, n_2 = 1.33$

This article has been accepted for publication in a future issue of this journal, but has not been fully edited. Content may change prior to final publication. Citation information: DOI 10.1109/JSEN.2019.2962610, IEEE Sensors Journal

The light path diagram in Fig.3 shows the light propagation inside the oblique end face fiber group. Because of the light-emitting angle, the path in the diagram is the borderline of a bunch of light. θ_i is determined by the geometry parameters of the sensor, α and θ. The restriction on the light traveling angle α comes from the light-emitting angle θ_s and total reflection condition of the fiber core and cladding. The restriction on the oblique angle θ comes from the optimal θ_i mentioned above and the backward direction of reflected light. Because the reflected light should propagate backward and should not leak out from the oblique surface, the maximum angle between the reflected light and the horizontal line, $\theta_r = 2\theta + \alpha$, should be less than 90°. Eq.(3) summarizes the relationship among α, θ_i, θ, where n_{core}, n_{clad} and n_{air} are the RI of fiber core, cladding and air, n_{core} is 1.63, n_{clad} is 1.51 and n_{air} is 1.

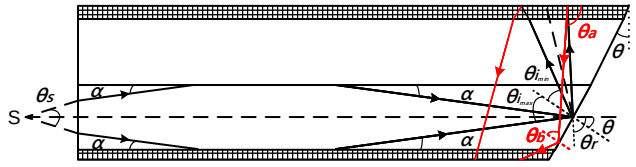

Fig. 3. Light path inside the oblique fiber group

The red line illustrates the light path of the reflected light coupling and backward traveling inside fibers. Some of the red lines reflected by the wall reach the oblique surface again. In order to protect them from escaping outside, their incident angle θ_b should be bigger than the critical angle. The relationship among the geometry angles is summarized in Eq.(4). After calculation of substituting Eq.(3) into Eq.(4), α is 2.9°, $\theta = \theta_{i_{\min}} + \alpha$ is 40.8°, and the range of θ_i is from 37.9° to 43.7°. According to the relationship between light emitting angle and light traveling angle, θ_s is 9.46°. Up to now, the geometry parameters of the sensor have been confirmed and $\theta_s = 9.46°$, $\theta = 40.8°$ guarantee a maximum reflected light intensity modulation. Because many groups of fibers are used to ensure large measurement range, the diameter of the emitting fiber bundle is as big as 1cm. Usually, the surface light source can be used to provide area lighting but its emitting angle is too big compared with $\theta_s = 9.46°$, which produces different reflection from expectation. A solution is the light pipe placed between fiber bundle and surface light source to absorb the light of big emitting angle.

$$\begin{cases} \theta_{i_{\max}} = \theta + \alpha \\ \theta_{i_{\min}} = \theta - \alpha = 37.9° \\ \theta_r = 2\theta + \alpha \le 90° \\ \alpha \le \begin{cases} \arcsin \dfrac{n_{air} \sin(\frac{\theta_s}{2})}{n_{core}} \\ \arccos \dfrac{n_{clad} \sin 90°}{n_{core}} \end{cases} \end{cases} \tag{3}$$

$$\begin{cases} \theta_a = \theta_r + 2 \times (90° - \theta_r) \\ \theta_b = 90° - (180° - \theta_a - (90° - \theta)) \\ \theta_b \ge \begin{cases} \arcsin \dfrac{n_{air} \sin 90°}{n_{core}} \\ \arcsin \dfrac{n_{liquid} \sin 90°}{n_{core}} \end{cases} \end{cases} \tag{4}$$

In order to measure the reflected light with a structure matched method, oblique receiving fibers are employed to interact with the reflected light inside emitting fibers based on side coupling effect, which makes easy detection. When a waveguide gets close to another, periodic exchange of energy between coupled waves takes place along the direction of wave propagation and eventually the two fibers have almost the same light. To validate the feasibility of this simultaneous interrogation method, the simulations of light path and light intensity detection by finite element analysis are performed. The prototype of calculation model is shown in Fig.4. Identical to the geometry parameters mentioned above, groups of emitting and receiving fibers are combined together on the 40.8° oblique surface. To simplify the model, each oblique fiber group has a light source and a photoelectric power meter at the flat end instead of only one light source and detector for all fibers. The incident light travels inside emitting fibers at the angle of $2\alpha = 5.6°$.

Fig.4b,4c shows the light path of light reflection and coupling inside the model with the help of COMSOL Multiphysics. When light propagates through the oblique end face, the reflected light behaves differently between fibers in the air and fibers in the liquid. In the air, all the incident lights are reflected back into emitting fibers and then are coupled into receiving fibers. But most incident lights leak out for the fibers in the liquid. All the reflected lights are coupled into receiving fibers and interrogated by the detector.

In Fig.5a, we set the time when the light sources start to emit light as the coordinate origin point and plot the interrogated light power as time goes by until the light power becomes stable. It is clearly shown that the reflected light power when fibers are totally in the air of 0.58mW is about 80 times as big as that when fibers are in the liquid of 0.0076mW, which confirms the modulation principle. The oblique angle θ_i is the major contributing factor to maximize light intensity modulation and the simulation of different θ_i around the optimal $\theta_i = 40.8°$ has been conducted to compare their modulation depth $R_{air} - R_{liquid}$. It is clear to find out in Fig.5b that the angle of 41° produces the maximum modulation, which coincides with the deduction. The received light power of different liquid levels is shown in Fig.5c. The light power becomes linear weaker when increasing the liquid level from bottom to top.

To sum up, the continuous level sensor measure liquid level according to the different reflected light intensity loss. An oblique end face with a specific oblique angle is employed to achieve the maximum refection difference. Such difference is interrogated with the help of receiving fibers. The feasibility of the structure has been confirmed by finite element analysis through COMSOL Multiphysics simulation.

This article has been accepted for publication in a future issue of this journal, but has not been fully edited. Content may change prior to final publication. Citation information: DOI 10.1109/JSEN.2019.2962610, IEEE Sensors Journal

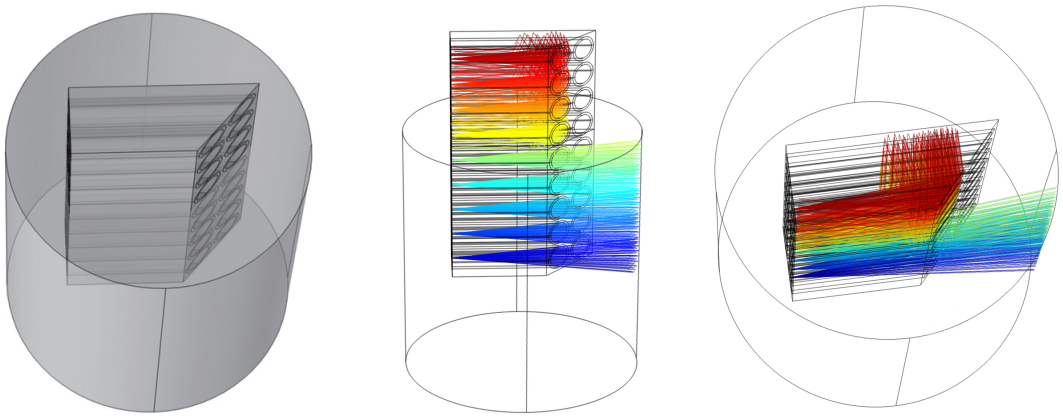

Fig. 4. Prototype of the oblique structure and light path simulation in COMSOL

III. Experiment

The experimental setup of the continuous level measurement is shown in Fig.6. There is a COB (chip on board) light source, a light power meter, a scaled container, a precise pump, and the liquid level sensor. The sensor is vertically attached on the wall of a liquid container. The light modulation element is the 5mm wide oblique surface with groups of oblique fibers vertically arranged on. Every group of emitting and receiving fiber is sealed by the shell with high reflectance to protect light inside from escaping outside. The height of the probe is the desired range of the sensor. When light from COB light source propagates into the emitting fibers, the light is restricted inside emitting fibers until it reaches the oblique end face where a part of light is reflected back into emitting fibers and then coupled into receiving fibers. The commercial light power meter (PM200 produced by ThorLabs) interrogates the reflected light intensity simultaneously and displays the value on the monitor.

The multi-mode silica fibers used in the sensor are produced by Nanjing Chunhui Science and Technology Industrial Co. Ltd. The multi-mode silica optical fiber has a diameter of 50um, with the RI of fiber core as 1.63 and the RI of fiber cladding as 1.51. Its numerical aperture is 0.64. The transmission efficiency of light intensity inside the fiber is $\geq 80\%$ per meter.

In the preparation stage, we keep the sensor vertically fixed on the container, run the sensor for 10 minutes before measuring liquid level, add liquid to the bottom of the sensor and adjust the light coupling to be optimal. Then, we can increase the liquid level with the help of a pump at a full speed of 0.13mm/s, and write down the output of light power meter corresponding to the level. The recording procedure will be repeated when decreasing the level.

IV. Results and Discussion

The performance of the sensor is attributable to many factors. In the experiments, the working conditions such as different RIs of the measured liquid and temperature are tested as well as the light fluctuation of light source and the property of the detector. The characteristics of the sensor, such as linearity, resolution, sensitivity, and stability, have been experimentally tested and improved to guarantee high performance.

To evaluate the characteristics of the sensor, a series of gradient level experiments have been conducted. The light power meter is PM200, a commercial optical power and energy meter produced by ThorLabs which works well within the temperature range from $-10°C$ to $70°C$ with high accuracy of $\pm 0.2\%$ full-scale and 16 bit analog-digital converter. In the process of increasing and decreasing liquid level in step of 1cm, the acquired reflected light power is recorded when it becomes stable. The procedure is repeated for 10 times and the average values of 10 light power data at each level have been calculated. It can be deduced from the results shown in Fig.7a,7b that the light power decreases when level increases, which is consistent with expectation. The uncertainty (difference between the measured output and the expected output marked as black line) at every level is expressed as the blue error mark on the black line. The maximum uncertainty is 0.0899mW at the level of 5cm in the level decreasing process and it is about 1.3% of the maximum output.

The reversibility of the sensor can be seen from the average output light power difference at the same level in the experiments of increasing and decreasing of the liquid levels shown in Fig.7c. Because of liquid residual on the oblique surface which reflects less light when fibers are in the air, the outputs at the same level in the increasing process are bigger than those in the decreasing process. The oblique surface and surface polishing are contributive to reduce the adhesion and the outputs have a maximum difference of 20uW which is small and acceptable compared with the output of operation. As a whole, the reversibility of the sensor is satisfactory as well as the hysteresis.

As summarized in Eq. (2), the sensitivity of the sensor is proportional to the modulation depth $M(\theta_i)$. Thanks to the maximum modulation depth optimal θ_i principle mentioned above, the sensitivity, corresponding to the slope of the curve

This article has been accepted for publication in a future issue of this journal, but has not been fully edited. Content may change prior to final publication. Citation information: DOI 10.1109/JSEN.2019.2962610, IEEE Sensors Journal

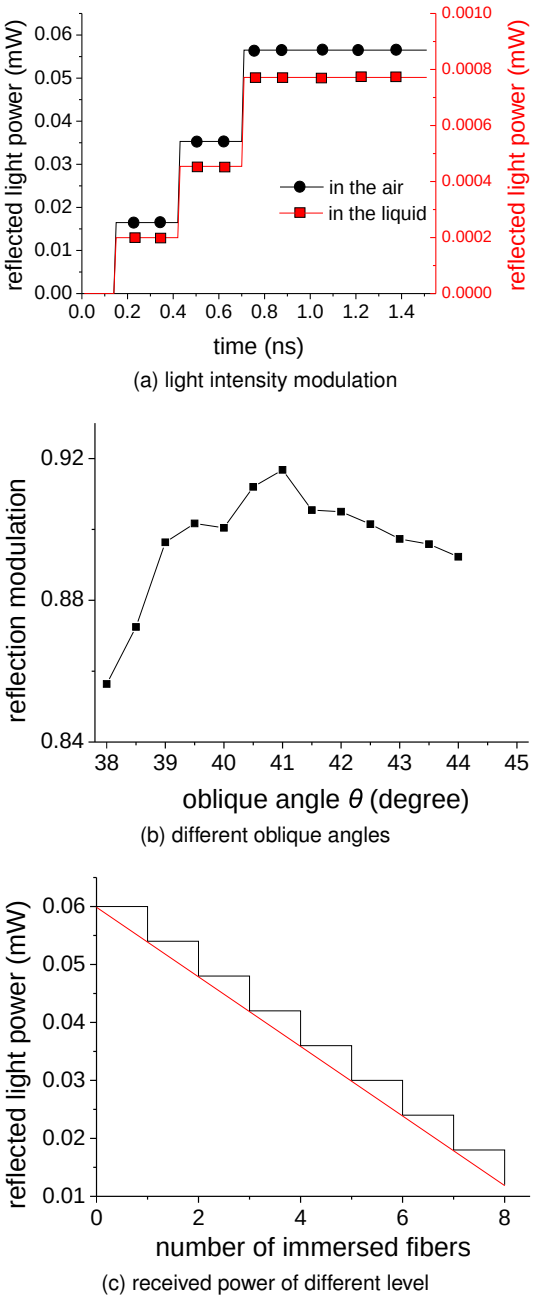

Fig. 5. Light intensity detection in COMSOL

shown in Fig.7a,7b, is as big as $0.21mW/cm$. The high sensitivity brings good resolution to the sensor. From 32mm to 37mm, a more slight gradient level experiment in step of 0.2mm has been conducted to find out the sensible minimum variance and the results are shown in the subfigures of Fig.7a, 7b. Because of the light source fluctuation of 10uW, only the output variance over 10uW caused by the level change is acceptable. A minimum level variance of 0.4mm is evidently sensed. As a matter of fact, the resolution of the sensor is related to not only the oblique angle θ_i of the oblique surface, but also the luminous power of the COB light source. A high power light source is helpful to increase the received effective light power caused by level variance and improve both sensitivity and resolution.

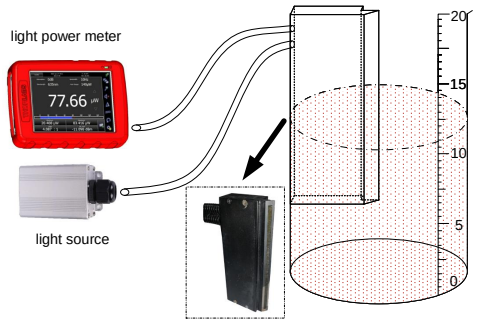

Fig. 6. Experimental setup for continuous level measurement

The output of the sensor is the sum of the reflected light power from submerged fibers and exposed fibers. Mathematically, according to $R_{total} = R_{air} - (R_{air} - R_{liquid}) \times h/H$, the reflected light power vs level is linear. The actual linearity of the sensor can be seen from the curves of acquired outputs drawn in black and fitting curves drawn in red in Fig.7a,7b. The linearity is poor. The situation is caused by the nonconsistency of the incident angle for every emitting fiber because the light source beam angle is big, which results in the small incident angle for center fibers while big incident angle for around fibers. Different incident angles lead to different reflections. A good solution to the nonlinearity is the mixture of fibers position by distributing the center fibers and around fibers all over the oblique surface instead of a gathering part and vice versa.

The influence of different liquid RIs has been tested by using water, 16.7% NaCl solution, and Jet A-1 fuel. The experimental results of increasing and decreasing the level every 1cm in different liquids are shown in Fig.8. At the start point when oblique fibers are exposed to the air, the reflected lights are almost the same. At the end point when oblique surface is totally immersed, the differences between different RIs are big. As expected, for the liquid with RIs of 1.33, 1.375 and 1.45, the liquid with higher RI has a weaker reflection at the same liquid level, because the liquid with higher RI reflects less light. Besides, the liquid with higher RI shows higher sensitivity according to the quicker attenuation of the curve of RI=1.45.

To test the stability of the sensor, a series of temperature shift, time drift, and light source stability experiments are carried out. In the temperature shift experiments, only the air and liquid are set to the specific temperatures, the light power meter and the light source are kept in room temperature. From 10°C to 70°C with step of 10°C, the outputs in Fig.9 show an obvious variance of 0.3mW, which equivalent to over 1cm level uncertainty. Because liquid RI and fiber transmission property generate different influences on the reflection of incident light at different temperatures, the effect of temperature is complex and interconnected with a variety of experimental conditions. From the principle of temperature and liquid RI, the rising temperature leads to the attenuation of liquid RI, which brings more reflection when the sensor works in the high temperature liquid. According

This article has been accepted for publication in a future issue of this journal, but has not been fully edited. Content may change prior to final publication. Citation information: DOI 10.1109/JSEN.2019.2962610, IEEE Sensors Journal

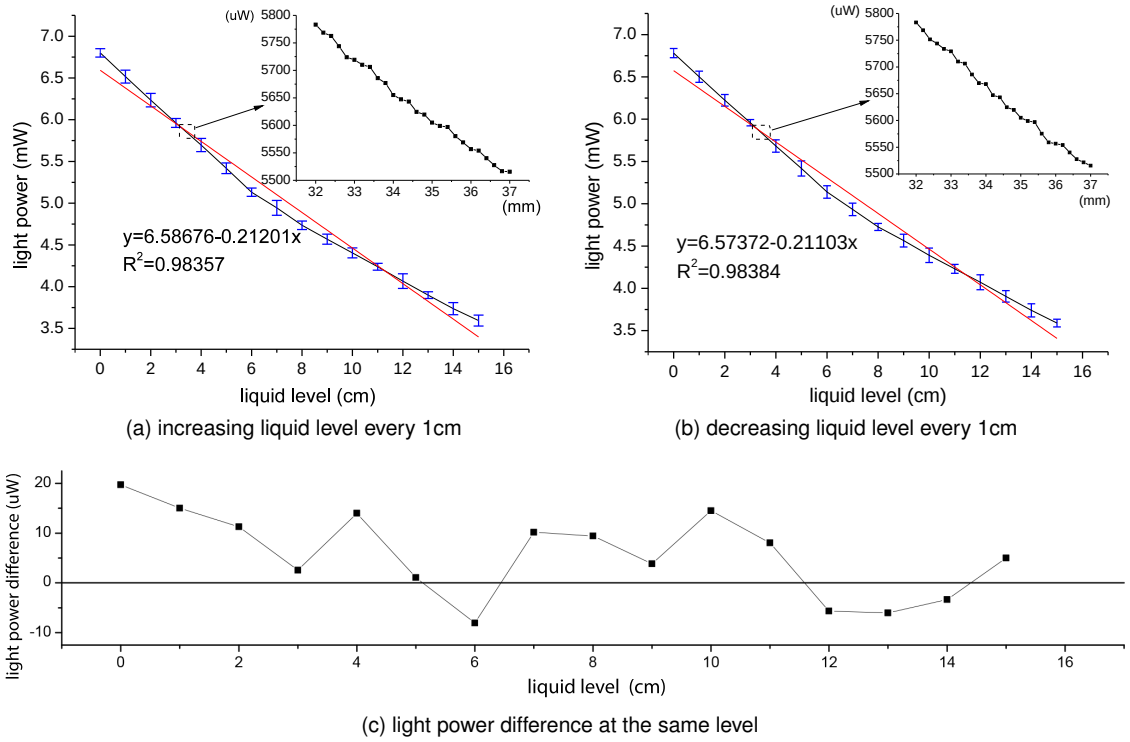

Fig. 7. Gradient level experiment in step of 10mm

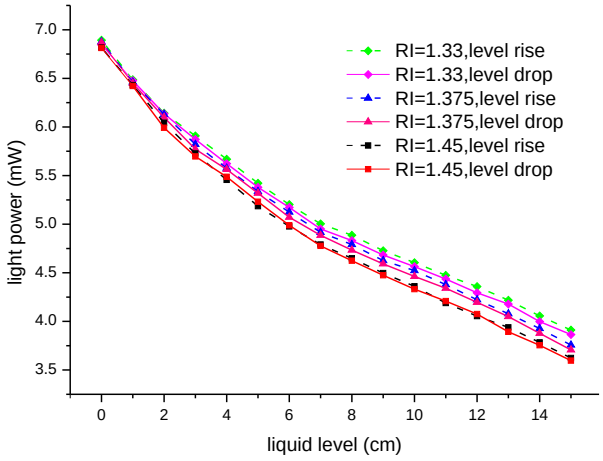

Fig. 8. The influence of different liquid: water, RI=1.33; 16.7% NaCl solution, RI=1.375; Jet A-1 fuel, RI=1.45

to the bottom curve in Fig.9a, when the sensor is totally immersed in the liquid, the output increases more quickly than half immersed, which follows Eq.(2). The output barely changes when the sensor is in the air because total reflection has occurred and the temperature shift makes no difference to the fiber transmission property. This experiment proves that the output is temperature dependent but the property of fiber is independent with temperature. The results of another experiment to test the influence of different temperatures on the output of the gradient level are shown in Fig.9b. In this experiment, liquid level increases and decreases at different temperature of 10°C,30°C,50°C,70°C. If temperature is higher, the output at the same liquid level is bigger and the sensitivity is smaller, which is identical to the effect of low RI liquid. Hence, the change of liquid RI caused by temperature plays the leading factor in the temperature shift. It can be deduced that the sensor is temperature independent except for the change of RI caused by environment temperature. Because of the linearity between RI and sensor output, the calibration of eliminating the effect of temperature is easy to realize.

Non-stop running for half an hour, the output voltage in Fig.10a gradually increases to a stable value of 3.25mW. According to the same variance trend of the light source beaming power in Fig.10b and received reflected light power in Fig.10a, it can be concluded that the time drift output is due to the shift of the COB light source. We have also investigated the property of the COB light source and found out that a pre-run time about 10 minutes is needed for the first start because the temperature around is affected by the COB, which in turn affects the light intensity until the temperature and light intensity come to a balance. Hence, turning on the light power 10 minutes before using it is a good way to achieve good stability. A further study of compensation for light source fluctuation will be focused. In the temperature shift and time drift experiments, the sensing capability and the health of oblique end face are not affected by temperature and other conditions. However, the environmental experiment with long time and severe conditions should be considered in the future.

V. Conclusion

An oblique fiber continuous level sensor based on the modulation of reflected light intensity has been proposed

This article has been accepted for publication in a future issue of this journal, but has not been fully edited. Content may change prior to final publication. Citation information: DOI 10.1109/JSEN.2019.2962610, IEEE Sensors Journal

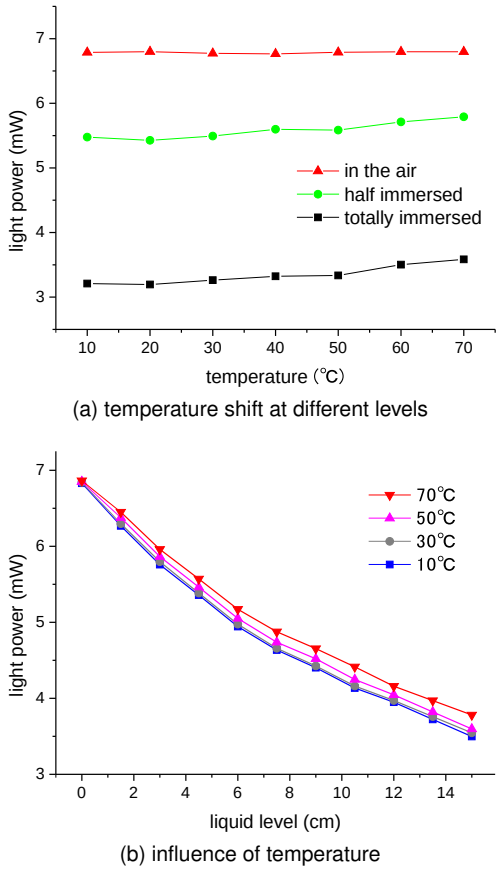

Fig. 9. Temperature shift experiments

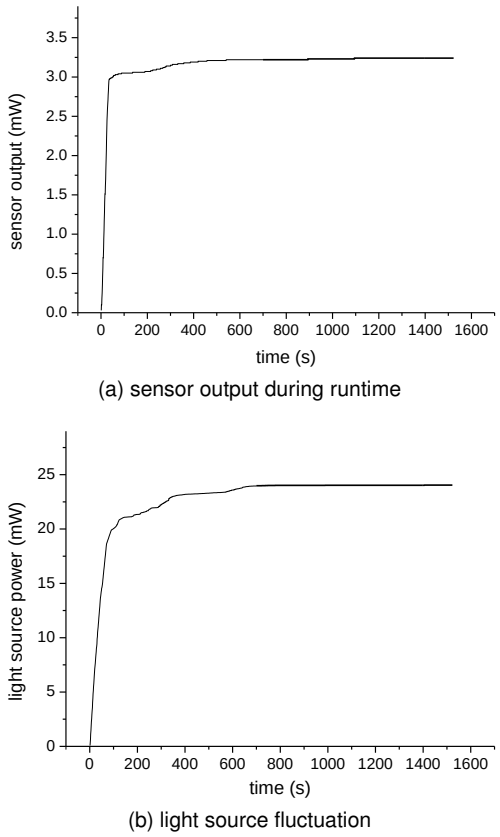

Fig. 10. Time drift of the sensor

and demonstrated. The sensor is constructed by vertically arranging groups of oblique fibers on the oblique surface, whose fabrication is simple and cost-effective. The oblique structure is the core of the sensor. The specific oblique angle deduced from the calculation model not only guarantees the maximum light modulation depth to improve sensitivity, but also reduces the droplet adhesion on the sensor surface. Besides, the reflected light from oblique surface can be detected by the side coupling effect with parallel attached receiving fibers. As the sum of the weak reflected light from immersed fibers and big reflected light from the fibers in the air, the acquired reflected light power is linear inversely proportional to level. A simulation by finite element analysis and a series of experiments confirm its feasibility and good stability. The sensor is sensitive to the variance of liquid level with the resolution of 0.4mm and high sensitivity of 0.21mW/cm.

Generally speaking, the proposed sensor, with a simple structure and regular equipments, archives pretty good performance in sensitivity, stability and anti-interference ability. The measurement range can be enlarged by reducing the width of the oblique surface. A better prospect in liquid level measurement is expected.

ACKNOWLEDGMENT

The authors would like to thank the anonymous reviewers for their valuable comments and suggestions which lead to an improvement of this paper.

REFERENCES

[1] R. Langton, C. Clark, M. Hewitt, and L. Richards, "Fuel system functions of commercial aircraft," in *Aircraft Fuel Systems*. Wiley Online Library, 2009, pp. 53–95.

[2] A. Abdel-Hafez, "Power generation and distribution system for a more electric aircraft - a review," in *Recent Advances in Aircraft Technology*. Rijeka: IntechOpen, 2012, ch. 13, pp. 289–308.

[3] P. Raatikainen, I. Kassamakov, R. Kakanakov, and M. Luukkala, "Fiber-optic liquid-level sensor," *Sensors & Actuators A: Physical*, vol. 58, no. 2, pp. 93–97, 1997.

[4] C. Yang, S. Chen, and G. Yang, "Fiber optical liquid level sensor under cryogenic environment," *Sensors & Actuators A: Physical*, vol. 94, no. 1, pp. 69–75, 2001.

[5] G. Onorato, G. Persichetti, I. A. Grimaldi, G. Testa, and R. Bernini, "Optical fiber fuel level sensor for aeronautical applications," *Sensors and Actuators A: Physical*, vol. 260, pp. 1–9, 2017.

[6] J. Ge, X. Cheng, K. Gui, W. Zhang, F. A. Cheikh, and L. Ye, "Oblique end face coupling optical fiber sensor for point fuel level measurement," *Sensors and Actuators, A: Physical*, vol. 297, p. 111505, 2019.

[7] K. E. Romo-Medrano and S. N. Khotiaintsev, "An optical-fibre refractometric liquid-level sensor for liquid nitrogen," *Measurement Science & Technology*, vol. 17, no. 5, pp. 998–1004, 2006.

[8] P. Nath, P. Datta, and K. C. Sarma, "All fiber-optic sensor for liquid level measurement," *Microwave & Optical Technology Letters*, vol. 50, no. 7, pp. 1982–1984, 2008.

[9] I. K. Ilev and R. W. Waynant, "All-fiber-optic sensor for liquid level measurement," *Review of Scientific Instruments*, vol. 70, no. 5, pp. 2551–2554, 1999.

[10] X. Dong and R. Zhao, "Detection of liquid-level variation using a side-polished fiber bragg grating," *Optics & Laser Technology*, vol. 42, no. 1, pp. 214–218, 2010.

[11] B. Yun, N. Chen, and Y. Cui, "Highly sensitive liquid-level sensor based on etched fiber bragg grating," *IEEE Photonics Technology Letters*, vol. 19, no. 21, pp. 1747–1749, 2007.

[12] Q. Jiang, D. Hu, and M. Yang, "Simultaneous measurement of liquid level and surrounding refractive index using tilted fiber bragg grating," *Sensors & Actuators A: Physical*, vol. 170, no. 1, pp. 62–65, 2011.

[13] Y. Wang, G. Yan, Z. Lian, C. Wu, and S. He, "Liquid-level sensing based on a hollow core bragg fiber," *Optics Express*, vol. 26, no. 17, pp. 21 656–21 663, 2018.

[14] S. Khaliq, S. W. James, and R. P. Tatam, "Fiber-optic liquid-level sensor using a long-period grating," *Optics Letters*, vol. 26, no. 16, pp. 1224–1226, 2001.

[15] A. A. Kazemi, C. Yang, and S. Chen, "Fiber optic cryogenic liquid level detection system for space applications," *Proc. SPIE, Photonics in the Transportation Industry: Auto to Aerospace II*, vol. 7314, pp. 73 140A–14, 2009.

[16] W. Feng and Z. Gu, "A liquid level sensor based on long-period fiber grating with superimposed dual-peak," *IEEE Photonics Technology Letters*, vol. 31, no. 14, pp. 1147–1150, 2019.

[17] J. E. Antonio-Lopez, J. J. Sanchez-Mondragon, P. LiKamWa, and D. A. May-Arrioja, "Fiber-optic sensor for liquid level measurement," *Optics Letters*, vol. 36, no. 17, pp. 3425–3427, 2011.

[18] Y. Ran, X. Li, D. Niu, Y. Wen, C. Yu, and D. Liu, "Design and demonstration of a liquid level fiber sensor based on self-imaging effect," *Sensors & Actuators A: Physical*, vol. 237, pp. 41–46, 2016.

[19] C. Li, T. Ning, C. Zhang, J. Li, X. Wen, L. Pei, X. Gao, and H. Lin, "Liquid level measurement based on a no-core fiber with temperature compensation using a fiber bragg grating," *Sensors & Actuators A: Physical*, vol. 245, pp. 49–53, 2016.

[20] Y. Tian, T. Tan, C. Duan, B. Xu, X. Zhao, Q. Chai, J. Ren, J. Zhang, E. Lewis, Y. Liu, J. Yang, and L. Yuan, "High sensitivity liquid level sensor based on dual side-hole fiber mach-zehnder interferometer," *Optics Communications*, vol. 440, pp. 194–200, 2019.

[21] S. Liu, J. Tian, N. Liu, J. Xia, and P. Lu, "Temperature insensitive liquid level sensor based on antiresonant reflecting guidance in silica tube," *Journal of Lightwave Technology*, vol. 34, no. 22, pp. 5239–5243, 2016.

[22] D. Liu, F. Ling, R. Kumar, A. K. Mallik, K. Tian, C. Shen, G. Farrell, Y. Semenova, Q. Wu, and P. Wang, "Sub-micrometer resolution liquid level sensor based on a hollow core fiber structure," *Optics Letters*, vol. 44, no. 8, pp. 2125–2128, 2019.

[23] Y. Dong, S. Xiao, H. Xiao, J. Liu, C. Sun, and S. Jian, "An optical liquid-level sensor based on d-shape fiber modal interferometer," *IEEE Photonics Technology Letters*, vol. 29, no. 13, pp. 1067–1070, 2017.

[24] L. Li, L. Xia, Z. Xie, and D. Liu, "All-fiber mach-zehnder interferometers for sensing applications," *Optics Express*, vol. 20, no. 10, pp. 11 109–11 120, 2012.

[25] G. Bawa, K. Dandapat, G. Kumar, I. Kumar, and S. M. Tripathi, "Single-multi-single mode fiber optic structure-based water depth sensor," *IEEE Sensors Journal*, vol. 19, no. 16, pp. 6756–6762, 2019.

[26] N. S. Fabián, A. B. Socorro-Leránoz, I. D. Villar, S. Díaz, and I. R. Matías, "Multimode-coreless-multimode fiber-based sensors: Theoretical and experimental study," *Journal of Lightwave Technology*, vol. 37, no. 15, pp. 3844–3850, 2019.

[27] A. S. Rajamani, M. Divagar, and V. Sai, "Plastic fiber optic sensor for continuous liquid level monitoring," *Sensors and Actuators A: Physical*, vol. 296, pp. 192–199, 2019.

[28] M. Lomer, A. Quintela, M. Lopezamo, J. Zubia, and J. M. Lopezhiguera, "A quasi-distributed level sensor based on a bent side-polished plastic optical fibre cable," *Measurement Science & Technology*, vol. 18, no. 7, pp. 2261–2267, 2007.

[29] C. Zhao, L. Ye, J. Ge, J. Zou, and X. Yu, "Novel light-leaking optical fiber liquid-level sensor for aircraft fuel gauging," *Optical Engineering*, vol. 52, no. 1, p. 4402, 2013.

[30] H. Zhang, L. Feng, Y. Hou, S. Shan, W. Liu, J. Liu, and J. Xiong, "Optical fiber liquid level sensor based on macro-bending coupling," *Optical Fiber Technology*, vol. 24, pp. 135–139, 2015.

[31] Y. Zhang, Y. Hou, Y. Zhang, Y. Hu, L. Zhang, X. Gao, H. Zhang, and W. Liu, "Continuous liquid level detection based on two parallel plastic optical fibers in a helical structure," *Optical Engineering*, vol. 57, no. 2, pp. 1–5, 2018.

[32] R. M. A. Azzam, "Relationship between the p and s fresnel reflection coefficients of an interface independent of angle of incidence," *Journal of the Optical Society of America A*, vol. 3, no. 7, pp. 928–929, 1986.

[33] M. Born and E. Wolf, "Electromagnetic potentials ans polarization," in *Principles of Optics: Electromagnetic Theory of Propagation, Interference and Diffraction of Light*, 7th ed. Cambridge: Cambridge University Press, 1999, ch. 2, pp. 71–108.

Junfeng Ge (S'08-M'09) received the B.S. degree in measurement and control technology and instrumentations from Huazhong University of Science and Technology (HUST), Wuhan, China, in 2003. He received the M.S. and Ph.D. degrees in control science and engineering from Tsinghua University, Beijing, China, in 2005 and 2009, respectively. He is currently an Associate Professor with the School of Artificial Intelligence and Automation, HUST. His research interests include ice detection, optical fiber sensor and instrumentation.

Xin Cheng received the B.S. degree in measurement and control technology and instrumentations from Huazhong University of Science and Technology, Wuhan, China, in 2018, where he is currently pursuing the M.S. degree. His research interests are in optical fiber sensors, aircraft fuel level sensor and intelligent hardware system.

Chengrui Zhao received the Ph.D. degree in control science and engineering from Huazhong University of Science and Technology, Wuhan, China, in 2013. He is now with the Research & Development Center, Ningbo CRRC Times Transducer Technology CO., LTD. His research interests include optical fiber sensors, measurement technology and instrumentation.

Kang Gui received the B.S. degree in measurement and control technology and instrumentations from Huazhong University of Science and Technology, Wuhan, China, in 2013, where he is currently pursuing the Ph.D. degree. His research interests are in road status sensors, multi-sensor data fusion, deicing system and road weather information system.

Wei Zhang received the B.S. degree in measurement and control technology and instrumentations from Huazhong University of Science and Technology, Wuhan, China, in 2003. He received the M.S. degree in control science and engineering from HUST, in 2006. He is currently a senior engineer with the Wuhan Second Ship Design and Research Institute. His research interests include control engineering and instrumentation.

Faouzi Alaya Cheikh received the B.S. degree in electronics from ENIT, Tunisia, in 1992. He received the M.S. and Ph.D. degrees in signal processing from Tshwane University of Technology, South Africa, in 1997 and 2004, respectively. He is currently a professor with the Department of Computer Science, Norwegian University of Science and Technology. His research interests include e-Learning, 3D imaging, image processing and video analysis, video-surveillance, biometrics, video-guided intervention and content-based retrieval. He is member of the Norwegian Colour and Visual Computing Laboratory (Colourlab).

Lin Ye received the M.S. degree from Huazhong University of Science and Technology, Wuhan, China, in 1988. From 1992 to 1993, he was a visiting scholar at Department of Automation, Moscow Institute of Power Engineering, Moscow, Russia. And from 1998 to 1999, he was a visiting scholar at Department of Aeronautics and Astronautics, Washington University, Washington, USA. From 2004, he has been a Professor with the School of Artificial Intelligence and Automation, HUST. His current research areas cover ice sensors, aircraft deicing system, in-situ emissivity measurement and non-contact temperature measurement.